Molecular Level Characterization of the Inorganic−Bioorganic Interface by Solid State NMR: Alanine on a Silica Surface, a Case Study

Ira Ben Shir,[†] Shifi Kababya,[†] Tal Amitay-Rosen,[‡] Yael S. Balazs,[†] and Asher Schmidt*[,†]

Schulich Faculty of Chemistry and Russell Berrie Nanotechnology Institute, Technion - Israel Institute of Technology, Technion City, Haifa 32000, Israel, and Chemical Physics Department, The Weizmann Institute of Science, Rehovot 76100, Israel

Received: January 6, 2010; Revised Manuscript Received: March 22, 2010

The molecular interface between bioorganics and inorganics plays a key role in diverse scientific and technological research areas including nanoelectronics, biomimetics, biomineralization, and medical applications such as drug delivery systems and implant coatings. However, the physical/chemical basis of recognition of inorganic surfaces by biomolecules remains unclear. The molecular level elucidation of specific interfacial interactions and the structural and dynamical state of the surface bound molecules is of prime scientific importance. In this study, we demonstrate the ability of solid state NMR methods to accomplish these goals. L-[1-^{13}C,^{15}N]Alanine loaded onto SBA-15 mesoporous silica with a high surface area served as a model system. The interacting alanine moiety was identified as the $-NH_3^+$ functional group by ^{15}N{^{1}H}SLF NMR. ^{29}Si{^{15}N} and ^{15}N{^{29}Si}REDOR NMR revealed intermolecular interactions between the alanine $-NH_3^+$ and three to four surface Si species, predominantly Q^3, with similar internuclear N···Si distances of 4.0−4.2 Å. Distinct dynamic states of the adsorbed biomolecules were identified by ^{15}N{^{13}C}REDOR NMR, indicating both bound and free alanine populations, depending on hydration level and temperature. In the bound populations, the $-NH_3^+$ group is surface anchored while the free carboxylate end undergoes librations, implying the carboxylate has small or no contributions to surface binding. When surface water clusters grow bigger with increased hydration, the libration amplitude of the carboxyl end amplifies, until onset of dissolution occurs. Our measurements provide the first *direct*, comprehensive, molecular-level identification of the bioorganic−inorganic interface, showing binding functional groups, geometric constraints, stoichiometry, and dynamics, both for the adsorbed amino acid and the silica surface.

Introduction

Binding and assembly of biomolecules onto inorganic surfaces are of major significance to a wide range of applications.[1−4] Protein adsorption and macromolecular interactions at solid surfaces play key roles in the performance of implants[4] and hard-tissue engineering.[5−8] DNA and proteins adsorbed specifically onto probe substrates have been used to build microarrays suitable for modern genomics,[9] pharmacogenetics,[10] and proteomics.[11,12] Although significant advances have been made in this area, many fundamental scientific questions are still to be answered. The design of functional interfaces between biomolecules and artificial surfaces requires a detailed, molecular level understanding of their interactions. Presently, the atomic/molecular details of inorganic−bioorganic interactions are limited and challenging to access.

Mesoporous silica materials are a class of synthetic materials with high surface area. Their synthesis (hydrolysis and condensation of silicate ions) in an aqueous solution in the presence of organic surfactants as templates leads to structures of amorphous silica that are periodic on the mesoscopic length scale.[13] MCM-41[14] and SBA-15[15] with pore diameters of 2−4 and 5−30 nm, respectively, are two well-known examples. The structure of mesoporous silicas has been studied extensively by X-ray[16−18] and neutron diffraction,[19,17] EPR,[20,21] transmission and scanning electron microscopy,[22] and solid state NMR,[23,24] making these materials relatively well-defined, and thus excellent model surfaces.

Presently, for addressing nanoscale interactions between biomolecules and inorganic surfaces, solid state NMR is one of the most insightful analytical tools.[25−30] High-resolution solid state NMR techniques, both newly developed and traditional, can provide structural and dynamical details at the atomic/molecular level of interfaces. The interfacial interactions unraveled by NMR are straightforwardly interpreted in terms of the chemical/physical principles that underlie the binding of the molecules to the surface.

Nevertheless, the study of interfacial interactions is nontrivial. One requirement is that NMR spectroscopy's inherently low sensitivity is optimized through stable isotope enrichment of the bioorganic molecules and high surface area inorganic materials such as SBA-15[15,31] and MCM-41.[14,32]

Vega and co-workers used solid state ^{1}H and ^{2}H MAS NMR to investigate the state (dynamics and structure) of water and alanine molecules adsorbed on a solid silica surface, SBA-15, as a function of the degree of surface hydration.[33] Their study identified two distinct alanine populations: (a) dynamic, molecules undergoing exchange between bound and free states; (b) static, surface "immobilized" isolated alanine molecules. Extracting the populations and the exchange rates, the thermodynamic parameters of alanine dissolution were determined. Interestingly, their study also reveals that a surprisingly small number of water molecules (>4 H/nm^2) is required for the onset

* To whom correspondence should be addressed. Phone: 972-4-8292583. Fax: 972-4-8295703. E-mail: chrschm@tx.technion.ac.il.
[†] Technion - Israel Institute of Technology.
[‡] The Weizmann Institute of Science.

10.1021/jp100114v
Published on Web 04/16/2010

of exchange, where surface immobilized alanines transfer to a solute-like environment with isotropic mobility. Remaining open questions pertain to the molecular level description of the surface binding itself, i.e., which functional groups of alanine and silica facilitate the binding, and how "static" are the surface bound alanine molecules. These questions set a prime goal for our study.

For this purpose, by probing NMR interactions with coupling strengths much smaller than the deuterium quadrupole coupling of the $-CD_3$ group (q_{cc} = 51 kHz), e.g., the intramolecular dipolar interactions $^{15}N\cdots{}^{13}C_1$ (~0.2 kHz) and $^{15}N-{}^{1}H_3$ (~3.9 kHz), the NMR experiments become sensitive to slower time scales than those explored by Vega and co-workers.[33] The change in time scales enables the scrutiny of both the binding details and the modes of local motions of bound alanine.

In the first part of this manuscript, we address the nature of alanine−SBA-15 interactions and the identity of both alanine and silica interacting moieties. This is accomplished using an L-[1-^{13}C,^{15}N]alanine loaded SBA-15 sample at a very low hydration level (<4 H/nm^2), and employing intermolecular alanine-surface dipolar recoupling experiments. In particular, the interacting moieties were identified and the binding geometry and stoichiometry were determined using intermolecular $^{15}N\{^{29}Si\}$ and $^{29}Si\{^{15}N\}$ rotational echo double resonance (REDOR)[34] and intramolecular, $^{15}N\{^{1}H\}$ dipolar recoupling separated local field (SLF)[35] NMR. The feasibility of *direct* identification of alanine−surface interactions is demonstrated here for the first time. Furthermore, using intramolecular dipolar recoupling experiments, $^{15}N\{^{13}C\}$ REDOR NMR, we elucidate the dynamic state of alanine molecules bound to the silica surface and determine the presence of different alanine populations and their distribution. In the last part, we investigate the influence of hydration level and temperature on the motional behavior of alanine.

Experimental Section

Materials. Specifically labeled compounds with stable isotope enrichment levels of 98% were used as received. L-[1- ^{13}C,^{15}N]-alanine and L-[u-^{15}N,^{13}C]lysine·2HCl were purchased from CIL (USA). [3-^{13}C,^{15}N]N-(Phosphonomethyl)glycine, Glp, was the kind gift of Prof. J. Schaefer from Washington University at St. Louis and used as received. SBA-15 (natural abundance ^{29}Si) was the kind gift of Prof. M. Landau, Ben-Gurion University. To directly relate our findings to those of Vega and co-workers,[33] and to avoid differences that may potentially occur during synthesis and sample preparation, we use SBA-15 silica from the same synthetic batch and employ the same loading procedure. The SBA-15 was characterized[33] by N_2 adsorption/desorption isotherm measurements with a NOVA-2000 (Quantachrome, version 7.01) apparatus. The surface area of 850 m^2/gr, pore volume of 11.3 cm^3/gr, and pore diameter of 159.1 Å were obtained from the isotherms using the BET and BJH methods. Micropores contribute only 3% to the surface area of the material and are therefore neglected.

Sample Preparation. Loading of 0.2 L-[1-^{13}C,^{15}N]alanine molecules/nm^2 on SBA-15 was previously reported by Vega and co-workers.[33] A 60 mg portion of calcined SBA-15, which was initially heated to 200 °C for 2 h (to remove residual water), was added to a 1.5 mL aqueous solution of 61 mg of L-[1-^{13}C,^{15}N]alanine (0.44 M). The suspension was stirred for 3 h at room temperature. The mixture was then filtered, and the remaining powder was allowed to dry in air. The remaining powder was then packed inside a 5 mm zirconia rotor with Teflon plugs and Vespel drive tip. The hydration level was reduced by exposing the sample inside the rotor (by removing its cap and top spacer) to a vacuum (10^{-3} Torr): pumping for 12 h yielded the "hydrated" state; extended pumping for 14 days yielded the "dry" state. Hydration level was raised by sample exposure to ambient atmosphere for limited time periods. The hydration state was estimated by comparison of ^{1}H MAS NMR spectra (recorded as a function of temperature) to those of Vega and co-workers.[33] The two hydration states of the sample considered in this manuscript, denoted "dry" (4 H atoms/nm^2) and "hydrated" (6−12 H atoms/nm^2), represent minute water content.

Solid State NMR. NMR spectroscopy measurements were carried out on a Chemagnetics/Varian 300 MHz CMX-infinity solid state NMR spectrometer equipped with three radio frequency channels and a 5 mm triple-resonance APEX Chemagnetics probe using 5 mm zirconia rotors. Samples were spun at 5000 ± 2 Hz throughout the experiments. Cross-polarization (CP) magic angle spinning (MAS) echo experiments (indirect excitation) were carried out with a 5.0 μs $\pi/2$, 10.0 μs π pulse widths, an echo interval τ (200 μs) identical to the rotor period T_R, a ^{1}H decoupling level of 100 kHz, and a relaxation delay of 1.5 or 2 s; Hartmann−Hahn rf levels were matched at 50 kHz, with a contact time of 1 ms for ^{15}N and 1.5 ms for ^{29}Si.

Direct ^{15}N excitation echo experiments, DE, were carried out with a 5.0 μs $\pi/2$, 10.0 μs π pulse widths, an echo interval τ equal to the rotor period T_R (200 μs), a ^{1}H decoupling level of 100 kHz, and a relaxation delay of 2 s. $^{15}N\{^{29}Si\}$, $^{29}Si\{^{15}N\}$, and $^{15}N\{^{13}C\}$ REDOR experiments were conducted using a REDOR pulse sequence with refocusing π pulses on each rotor period (T_R) on the observed channel and dephasing π pulses in the middle of each rotor period on the nonobserved nuclei, followed by an additional two rotor periods with a chemical shift echo π pulse in the middle. REDOR π pulses employed xy8 phase cycling for the refocusing and recoupling pulses.[34,36] Data acquisition employed an alternating block scheme, collecting a single S_0 transient with recoupling pulses turned off, followed by S_R transient collection with recoupling pulses turned on. REDOR difference data obtained via $S_0 - S_R$ subtraction yield spectra which exclusively exhibit peaks of dipolar-coupled chemical species. All REDOR data presented in the figures were collected using the CP excitation scheme. A representative set of experimental $^{15}N\{^{29}Si\}$ REDOR data points were also measured for both "dry" and "hydrated" states, employing the DE excitation scheme. The resulting DE-REDOR data (not shown) overlapped with CP-REDOR data, hence confirming that all alanine populations are correctly reported by the CP excitation. The number of collected transients was set to yield an adequate signal-to-noise ratio; typical numbers of transients are 2048 and 10240 for experiments detecting ^{15}N and ^{29}Si, respectively.

The chemical shifts of ^{15}N and ^{29}Si are reported relative to solid $(^{15}NH_4)_2SO_4$ and TMS, respectively. Simulations and fitting of REDOR data were performed using SpinEvolution.[37] Peak areas were calculated by deconvolution using DMFIT.[38]

The SLF solid state NMR technique was modified to include the phase modulated Lee−Goldburg (PMLG5)[39−43] homonuclear decoupling. PMLG5 allows the efficient removal of homonuclear dipolar interactions between abundant hydrogen atoms. Specifically, the odd dipolar-rotational spin−echo (ODRSE) experimental scheme of Bork et al. was used.[44] In this experimental scheme, during the rotor-synchronous echo formation of the magnetization generated by cross-polarization, the magnetization is allowed to evolve under the influence of scaled heteronuclear dipolar coupling during a variable time which is incremented

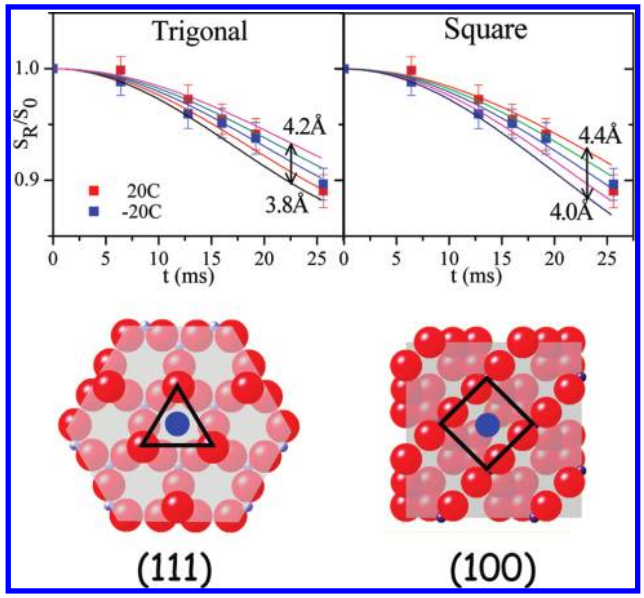

Figure 1. Bottom: Top view of (111) (left) and (100) (right) crystal planes of β-crystobalite with an N-atom (blue, representing alanine amine) centered above triangular and square, respectively, planar arrangements of Si atoms (purple). A surface silicon atom is present below each corner of the black triangle and square. The red circles represent oxygen atoms. Top: Experimental $^{15}N\{^{29}Si\}$ REDOR dipolar evolution data of L-[1-^{13}C,^{15}N]alanine loaded on SBA-15 in the "dry" state at temperatures of −20 and 20 °C. Simulated REDOR curves for different N···Si distances that span the width of the experimental error are normalized to maximum relative attenuations of 14.1 and 18.8% for the trigonal (left) and square (right) pyramid models, respectively.

between zero and two rotor periods ($2T_R$). The reintroduction of the heteronuclear dipolar coupling is facilitated by suppression of the $^1H-^1H$ homonuclear dipolar coupling employing PMLG5. The echo π pulse on the rare nuclei at the completion of the first rotor period (center of the H−X recoupling period) refocuses chemical shifts at the completion of the second rotor period.[45] The PMLG5 experiment was optimized first on natural abundance adamantane looking for the best resolved C−H ^1J-splitting. The experimental parameters of the optimized PMLG5 cycle employed on-resonance ^1H irradiation with a 1.9 μs pulse width, 90 kHz rf level, 0.1 μs delay for phase setting, and an overall cycle time of 20 μs.

Results

Bioinorganic Interface: Alanine−Silica Surface Interactions, "Dry" State. The results for SBA-15 loaded with L-[1-^{13}C,^{15}N]alanine at the least hydrated state, with a surface density of <4 H atoms/nm^2, are described first. Characteristic ^{13}C and ^{15}N CPMAS spectra are shown in the Supporting Information.

Alanine Nitrogen Proximity to Silica Silicon. CP $^{15}N\{^{29}Si\}$ REDOR experiments, which probe for $^{15}N\cdots^{29}Si$ proximities of up to 5 Å, are employed to identify the occurrence of silica−alanine interfacial interactions. The application of $^{15}N\{^{29}Si\}$ REDOR to the sample in the "dry" state gives rise to S_0 and S_R spectra with a single ^{15}N peak from the ^{15}N-enriched L-alanine. Monitoring the relative intensity of the ^{15}N peak (S_R/S_0), its decrease is clearly observed as the recoupling period is extended from 32 to 128T_R (Figure 1, top). This measurable $^{15}N\cdots^{29}Si$ REDOR evolution shows a finite $^{15}N\cdots^{29}Si$ dipolar interaction, indicating the occurrence of interfacial interactions where alanine molecules are bound to the SBA-15 surface via their amine moiety. In a situation in which an alanine nitrogen atom is proximate to a single surface Si atom, the probability of the latter being ^{29}Si is 4.7%, its natural abundance. Therefore, in this case of isolated $^{15}N\cdots^{29}Si$ nuclei pairs, the maximum possible REDOR signal attenuation is 4.7%. The observed ~11% attenuation of the relative REDOR signal, S_R/S_0, at the longest measured recoupling time ($N = 128$, $t = 25.6$ ms), being greater than the natural abundance of ^{29}Si, reflects the nature of the surface binding site: *more than two* surface Si atoms must be proximate to the alanine nitrogen atom. Only then, the probability for a single ^{29}Si isotope nearby the nitrogen is increased, and accordingly the maximum possible attenuation of the ^{15}N peak. For example, in the case of amine proximity to three Si atoms, the total probability that one of them is ^{29}Si, is 3 × 4.7% = 14.1%; similarly, proximity to four Si atoms will have 4-fold probability of 4 × 4.7% = 18.8%. These percentages, being the probabilities for the occurrence of isolated $^{15}N\cdots^{29}Si$ pairs, also reflect the respective maximum REDOR attenuation for each such geometric arrangement. In such possible $N\cdots Si_n$ arrangements, the relative probability for the presence of $^{15}N\cdots^{29}Si_2$ is below 15% of that of the isolated $^{15}N\cdots^{29}Si$ pairs for $n \leq 4$ (thus, in absolute terms, less than 0.8% of the overall peak intensity). This contribution to the REDOR results is within the noise and will be ignored in the following analysis.

For the quantitative analysis of our REDOR data, we refer to the crystalline (111) and (100) facets of β-cristobalite,[46] reported to have surface characteristics close to amorphous silica.[47,48] These two facets expose trigonal (111) and square (100) geometries of surface silanol groups, both with shortest Si···Si distances of 5.07 Å (Figure 1, bottom). For the data analysis, we will consider two geometric arrangements formed by placing the alanine nitrogen centered above the three or four surface Si atoms, respectively, such that the ^{15}N nucleus is at the head of either a trigonal or square pyramid and equidistant from the Si atoms. A top view of such geometries is shown in Figure 1, bottom. Although the SBA-15 under investigation consists of amorphous silica, the occurrence of similar surface geometric arrangements with varying degree of distortion/disorder is highly probable. It is noted that the two crystalline facets expose different species, Q^3 by the (111) and Q^2 by the (100), yet these functional groups may not be preserved in the amorphous mesoporous silica.

Considering a single population of bound alanine molecules (*vide infra*), the N···Si internuclear distance for isolated $^{15}N\cdots^{29}Si$ pairs is readily determined for each of the two geometric models by best fitting the experimental data with simulated REDOR evolution.[37] The plotted S_R/S_0 REDOR evolution curves (Figure 1, top) account for the maximum possible REDOR attenuation of 14.1 and 18.8% for the trigonal and square pyramids.

The best fit REDOR evolution curves yield $^{15}N\cdots^{29}Si$ dipolar coupling strengths of 38 and 33 Hz (three and four Si neighbors), corresponding to $r[N\cdots Si]$ values of 4.0 ± 0.2 and 4.2 ± 0.2 Å. The vertical position of the N-atom above the plane of the three or four Si atoms (the heights of the pyramids) is readily calculated, yielding 2.8 or 2.3 Å, respectively.

Varying the experimental temperature at which the $^{15}N\{^{29}Si\}$ REDOR data is acquired (−20 and 20 °C) does not change the REDOR decay nor the best fit parameters of the data (Figure 1, legend). This means that the N···Si internuclear distance has not increased with an increase in temperature over the given range. This temperature insensitivity implies strong alanine to SBA-15 surface interactions.

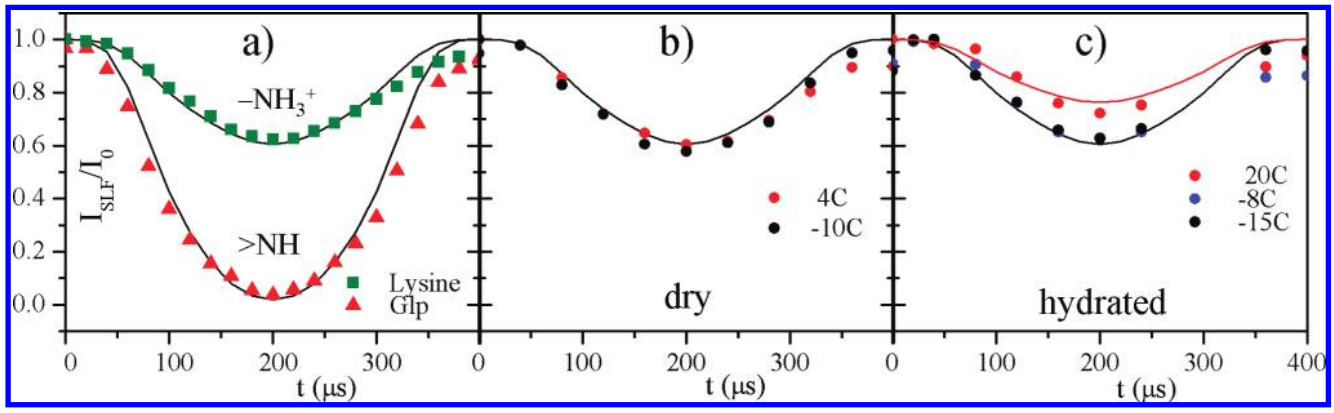

Figure 2. Experimental $^{15}N\{^1H\}$ SLF[PMLG5] dipolar evolution of the ^{15}N peak intensity as a function of homonuclear decoupling time *t*. (a) Two model compounds: >NH group of Glp (▲) and $-NH_3^+$ group of Lys·2HCl (■); data were recorded at 4 °C. Simulations (curves) were performed using a dipolar scaling factor of 0.58 and N−H dipolar couplings of 11.4 and 11.8 kHz for >NH and $-NH_3^+$ (1.04 and 1.01 Å). For the latter, the simulation accounted for the C_3 rotation of $-NH_3^+$. (b) "Dry" and (c) "hydrated" L-[1-^{13}C,^{15}N]alanine on SBA-15 as a function of temperature. The $-NH_3^+$ simulation (as in part a) fits the experimental data of the "dry" state at both temperatures, and that of the "hydrated" state at the two lowest temperatures. For the hydrated state at 20 °C, the fit employs the same dipolar parameters, however, corrected by a contribution from a population, 40%, of free (rapid, isotropic reorienting) alanine molecules (dissolved) and, hence, with vanishing N−H coupling.

Protonation State of Bound Alanine Amine, SLF Experiments. A question of prime interest is the protonation state of the surface bound amine moiety of alanine. Addressing this question experimentally can be a formidable task. We chose to pursue the application of a separated local field (SLF) experiment[35,44] combined with PMLG5 homonuclear decoupling[39−43] to efficiently remove the strong homonuclear dipolar interactions between abundant hydrogen atoms. The $^{15}N\{^1H\}$ SLF experiments directly correlate the observed intranuclear $N-H_{(n)}$ dipolar interaction strength within the N-amino group and its structural and dynamical properties, i.e., mobility and chemical environment.[45,49] To devise this $^{15}N\{^1H\}$ SLF[PMLG5] solids NMR methodology, we exploited two specifically labeled model compounds: L-[u-^{15}N,^{13}C]lysine·2HCl and [3-^{13}C, ^{15}N]N-(phosphonomethyl)glycine (Glp).

Typical dipolar evolution curves were measured for each of the two model compounds of the reference set at 20 °C: the static >N−H group of Glp and the freely rotating charged $-NH_3^+$ group of L-[u-^{15}N,u-^{13}C]lysine·2HCl (Figure 2a). This figure shows the intensity modulation of the (labeled) ^{15}N peaks as a function of homonuclear decoupling time, t_1. The rapid rotation of the $-NH_3^+$ averages the $^{15}N-^1H$ dipolar interaction, hence resulting in a shallower dipolar SLF curve compared to that of the static glyphosate >NH group. Experimental results are supported by theoretical simulations (Figure 2a, solid line) using a N−H dipolar coupling of 11.4 kHz for >N−H (1.04 Å N−H bond length) and 11.8 kHz for $-N-H_3^+$ (1.01 Å). The fast C_3 rotation of the $-NH_3^+$ group scales the N−H dipolar coupling by a factor of 0.34, yielding 3.88 kHz.[50,51] The theoretical Lee−Goldburg scaling factor of 0.58[39,43] was used for the two simulated curves, both showing excellent agreement with the experimental data. The small deviations of the experimental data from the theoretical curve in the second half of the dipolar SLF evolution are commonly observed[45] and attributed to either imperfections of the homonuclear decoupling, T_2 relaxation processes, or intermediate dynamic processes.

Conducting the same measurements for the SBA-15 surface bound alanine ("dry" state) yields a dipolar SLF curve that overlaps that of lysine·2HCl and the $-NH_3^+$ simulated curve, hence identifying alanine's binding moiety as the freely rotating charged ammonium group, $-NH_3^+$ (Figure 2b).

Silica Surface Species Interacting with Alanine, $^{29}Si\{^{15}N\}$ REDOR. Characterization of the surface using cross-polarization (experimental) selects ^{29}Si moieties proximate to ^{1}H nuclei,

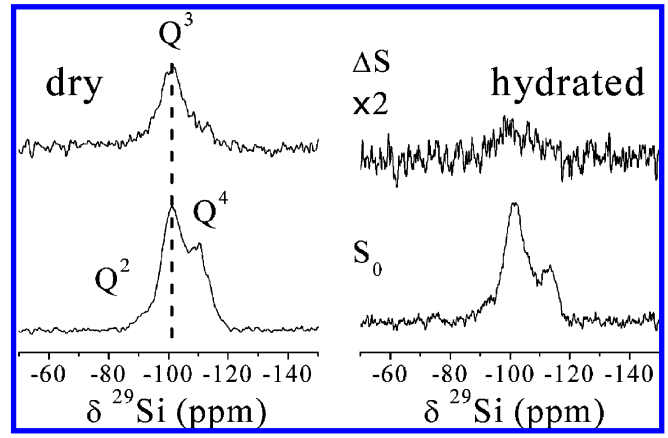

Figure 3. $^{29}Si\{^{15}N\}$ $128T_R$ (25.6 ms) REDOR spectra of L-[1-^{13}C,^{15}N]-alanine loaded onto SBA-15 in the "dry" (left) and "hydrated" states (right). Dephasing of the Q^3 species dominates the difference spectra (ΔS, top), identifying it as the preferential surface functional group that binds *N*-ammonium of alanine. Difference spectra are drawn normalized relative to their respective reference spectra. The normalized, total integrated intensity of the "hydrated" reference spectrum is twice larger than that of the "dry" S_0 spectrum. Spectra were recorded at 4 °C.

hence emphasizing species present on the SBA-15 silica surfaces. This selection is further emphasized at populated binding sites, where hydrogen atoms of alanine contribute to the CP a significant fraction (a third) of the proton density (7 H/alanine × 0.2 alanine/nm^2 = 1.4 H/nm^2 out of <4 H/nm^2). The reference $^{29}Si\{^{15}N\}$ REDOR spectrum (Figure 3, S_0) shows Q^2 (Si*$(OSi)_3(OH)_2$), Q^3 (Si*$(OSi)_3OH$), and Q^4 (Si*$(OSi)_4$), with Q^3 dominating the spectrum in accordance with its identification as a primary surface species.[47,52] Moreover, $^{29}Si\{^{15}N\}$ REDOR experiments applied to the "dry" sample clearly show a difference peak predominantly for the Q^3 species (Figure 3, left). Deconvolution of the REDOR spectra (not shown) shows a 26% REDOR attenuation overall, with the relative attenuation of the Q^3 peak being about 3 times larger than that of Q^4, S_R/S_0, at the longest recoupling time ($128T_R$, 25.6 ms). These observations further confirm that the alanine molecules are bound to the SBA-15 surface (via their ammonium moiety, above), and show that interacting surface sites are predominantly Q^3 sites. Fitting the $^{29}Si\{^{15}N\}$ REDOR data (not shown) assuming isolated pairs of nuclei with a dipolar coupling of 35 Hz, as found by the analysis of the $^{15}N\{^{29}Si\}$

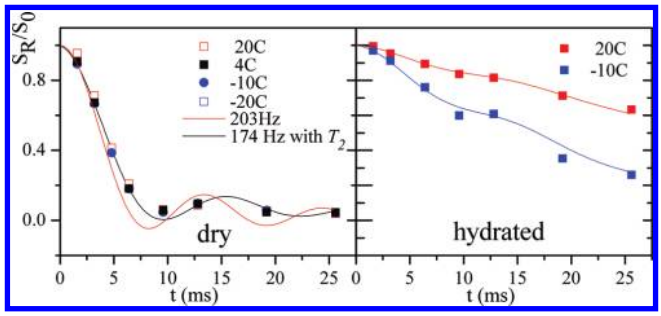

Figure 4. Intramolecular $^{15}N\{^{13}C\}$ S_R/S_0 REDOR evolution at different temperatures for L-[1-^{13}C,^{15}N]alanine loaded onto SBA-15, "dry" (left) and "hydrated" (right) states, at different temperatures. Continuous curves represent REDOR simulations. Left: Red and black curves were calculated for dipolar $^{15}N\cdots^{13}C$ couplings of 203 Hz (2.45 Å) and 174 Hz; the latter was further apodized with an exponential "T_2" decay of 40 ms (8 Hz line broadening) (black). Right: Continuous curves were generated by adding three calculated REDOR dipolar evolutions with three distinct populations, as detailed in Table 1.

TABLE 1: $^{15}N\cdots^{13}C_1$ Dipolar Couplings and Populations at the Two Temperatures Obtained from Fitting the $^{15}N\{^{13}C\}$ REDOR Data for the Sample in the "Hydrated" State (Figure 4, Right)[a]

−10 °C		+20 °C	
25%	174 Hz	10%	174 Hz
58%	44 Hz	50%	34 Hz
17%	0 Hz	40%	0 Hz

[a] The populations and coupling strengths are determined within ±10% and ±10 Hz, respectively.

REDOR data, shows that full dephasing should be reached at a level of ∼45%. This indicates that ca. 45% of the surface Si atoms reported by the CP experiment are within 4.0−4.2 Å of a ^{15}N atom of alanine.

If all surface Si atoms were equally reported by the cross-polarization experiment, and considering an alanine loading of 0.2 alanine molecules/nm^2 (experimental) and average Si surface density of 4.6 Si/nm^2,[53] the maximum possible $^{29}Si\{^{15}N\}$ REDOR dephasing is 4.5%. This value being only $^1/_{10}$ of the total dephasing (∼45%) further confirms that in the "dry" state the ^{29}Si CP experiment emphasizes populated surface binding sites, leaving a significant surface area with ineffective cross-polarization.

Molecular Motion and Dissolution of Surface Bound Alanine. ***"Dry" State, Single Population.*** Characterization of alanine dynamics is achieved by monitoring the intramolecular $^{15}N\cdots^{13}C_1$ dipolar coupling in L-[1-^{13}C,^{15}N]alanine. Its fixed internuclear $^{15}N\cdots^{13}C_1$ distance of 2.473 Å[54] translates to a dipolar coupling strength of 203 Hz, for which the calculated REDOR S_R/S_0 evolution is shown by the continuous curve in Figure 4 (left). The measured $^{15}N\{^{13}C\}$ REDOR data (Figure 4, left, squares) show a slightly slower decay, best fit by a REDOR curve of 174 Hz coupling strength and apodized with a T_2 exponential decay of 40 ms (8 Hz). This 14% reduction of the static dipolar coupling is interpreted in terms of averaging of the $^{15}N\cdots^{13}C_1$ dipolar interaction via fast, small amplitude, anisotropic motion of the intramolecular $^{15}N\cdots^{13}C_1$ vector. The need to apodize with a 40 ms decay is rationalized by the presence of an additional slow motion (∼8 s^{-1}).

It should be noted that, for L-[1-^{13}C,^{15}N]alanine in a molecular crystal, Schaefer and co-workers reported a $^{15}N\{^{13}C\}$ REDOR measured dipolar coupling of 189 Hz, i.e., 5% reduction compared to the crystal structure value;[55] this reduction was attributed to fast, small amplitude librations.

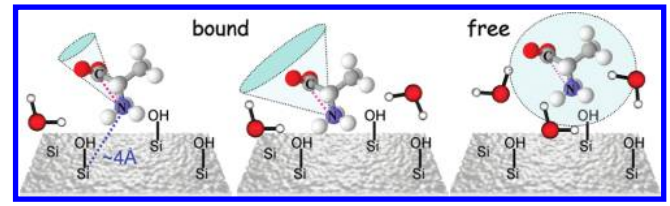

Figure 5. Schematic representation of the three distinct geometric-dynamic states of alanine loaded onto SBA-15 at the "hydrated" state (6−12 H atoms/nm^2). The left-most and center schematics represent bound, ammonium anchored alanine, with its carboxylate end undergoing rapid anisotropic reorientation. The right-most graphic represents onset of dissolution, with alanine undergoing rapid, isotropic reorientation.

Repeating the REDOR experiments at four different temperatures, −20, −10, 4, and 20 °C, shows negligible differences (Figure 4, left). This absence of temperature dependence is, as in the case for the $^{15}N\{^{29}Si\}$REDOR experiments (Figure 1), probing the intermolecular inorganic−organic interactions. This stable, relatively rigid, and unperturbed binding (within the 40 °C temperature range examined) further confirms that alanine is tightly bound to the SBA-15 surface.

The physical picture that emerges from the accumulated data at the lowest hydration state is that of a single population of all likely bound alanine molecules, anchored to the silica surface via their positively charged ammonium moiety; simultaneously, the carboxylate end of the molecules undergoes small amplitude, fast libration. The ammonium moiety interacts with the surface site consisting of three to four surface Si atoms, with Q^3:Q^4 of ∼3:1.

Effect of Increased Hydration, Three Alanine Populations. To investigate the effect of hydration on the alanine molecules adsorbed onto the SBA-15 silica, we examined a hydrated sample with an estimated surface hydrogen density of 6−12 H atoms/nm^2 versus <4 H/nm^2 for the "dry" state described thus far. Note that for both samples the quantity of water present is miniscule.

In contrast to the REDOR evolution for the "dry" state, $^{15}N\{^{13}C\}$ REDOR data for the "hydrated" sample exhibit much slower and partial decays (Figure 4). This indicates that more pronounced, yet anisotropic dynamics of the $N\cdots C_1$ internuclear vector occur. The change of the REDOR decay curve when a small amount of water is present is dramatic for both temperatures measured (−10 and +20 °C). Moreover, the dipolar REDOR evolution data at both temperatures can no longer be fit by a single dipolar coupling evolution.

In an attempt to fit the data, we assume the presence of three alanine populations with distinct dipolar coupling strengths, with three being the smallest possible number of populations. In each population, alanine molecules undergo different dynamics, hence leading to a differently averaged dipolar interaction. We also assume that all dynamic processes are at the fast limit compared to the inverse dipolar coupling strength (5 ms). Very good fits to the data are achieved by assuming the values shown in Table 1. At each temperature, there exist two populations with finite dipolar couplings that correspond to alanine molecules that undergo restricted motion: the 174 Hz population corresponds to that seen in the "dry" state, while the population with the further averaged dipolar interaction (33−44 Hz) represents alanine molecules undergoing larger amplitude motion. A third population with averaged to zero dipolar coupling consists of alanine molecules that undergo rapid isotropic reorientation. A schematic representation of the three dynamic states is shown in Figure 5. The first two, with finite dipolar couplings,

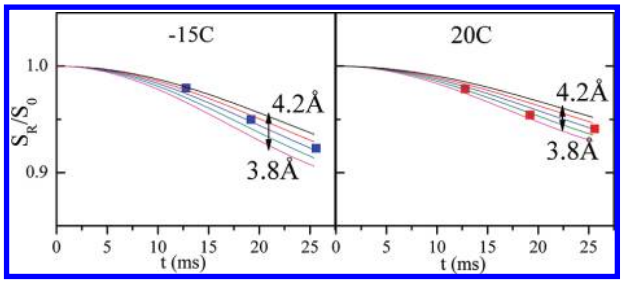

Figure 6. Experimental $^{15}N\{^{29}Si\}$ REDOR evolution of L-[1-^{13}C,^{15}N]-alanine loaded onto SBA-15 in the "hydrated" state at two temperatures −15 (left) and 20 °C (right). Simulated curves are for a set of $^{15}N\cdots^{29}Si$ distances (dipolar couplings) normalized to maximum dephasing of 14.1% as in the trigonal pyramid model, and accounting for a population of free alanine molecules (rapid, isotropic reorientation) with a vanishing $^{15}N\cdots^{29}Si$ coupling strength. The free population makes up 20% of the total alanine load at −15 °C and 40% at 20 °C.

correspond to bound populations, while the third is attributed to a "free" population of solvated alanine molecules.

Protonation State of Alanine Amine at Increased Hydration, SLF Experiments. The $^{15}N\{^{1}H\}$ SLF experiment applied to the hydrated sample at the reduced temperatures of −15 and −8 °C gives rise to the data shown in Figure 2c, right. The SBA-15 surface bound alanine with increased hydration exhibits just a slightly shallower evolution than the dry sample (Figure 2b), yet it remains very similar to the experimental data (model compound) and theoretical analysis of the $-NH_3^+$ moiety. Thus, the alanine amine at these conditions is also identified as the freely rotating $-NH_3^+$ (Figure 2a). At these temperatures, the $^{15}N\{^{13}C\}$ REDOR experiments were well fit by two bound alanine populations totaling 83% (58% + 25%) and a 17% rapidly isotropic reorienting population (Table 1). The rapid isotropic reorientation of molecules within the latter population would lead to complete averaging of the N−H dipolar coupling; hence, the $^{15}N\{^{1}H\}$SLF curve should reach 0.67 rather than 0.6. The experimental data at −15 and −8 °C are indeed slightly shallower, in accordance with the above analysis.

At the higher temperature of 20 °C, where the population of the free alanine increases, the resulting SLF evolution is significantly shallower (Figure 2c). This fact is straightforwardly rationalized in view of our $^{15}N\{^{13}C\}$ REDOR observation at 20 °C, showing the presence of a free alanine population, 40%, that undergoes rapid isotropic motion (Table 1). Had this isotropic motion been faster than 3.88 kHz, the N−H dipolar coupling, it would result in its complete averaging, and the SLF evolution would reach a minimum value of 0.76 instead of 0.6 (as for the single "dry" population). The experimental SLF data reach an intermediate value of ∼0.7. This fact therefore indicates that, with respect to the N−H coupling, fast limit averaging does not occur for the entire "free" population. The above observations further substantiate the identification of the two bound alanine populations being anchored via their $-NH_3^+$ moiety also at 20 °C. This anchoring acts as a pivot point with the $N\cdots C_1$ vector reorienting either with a small or larger amplitude motion, yet without further averaging the $-N-H_3^+$ coupling.

Bioinorganic Interfacial Interactions at Increased Hydration. ***Alanine Nitrogen Proximity to Silica Silicon.*** CP $^{15}N\{^{29}Si\}$ REDOR data at −15 and 20 °C show (Figure 6) significant attenuation (8 and 6% at the longest recoupling) yet smaller than the 11% observed for the "dry" state (Figure 1). This change is expected in view of our identification of a significant "free" population found for the "hydrated" state. Quantitative analysis of the data sets at the two temperatures is done by optimizing simulated REDOR curves that account for our previous observations. The free alanine population at 20 °C is 40%; at −15 °C, it is estimated from the measured value at −10 °C and taken as ∼20%. For this free population, the $^{15}N\cdots^{29}Si$ dipolar coupling is fully averaged out by the reorientation. For the remaining alanine population, binding is assumed to be identical to the "dry" state with a $^{15}N\cdots^{29}Si$ distance of 4.0 ± 0.2 Å (38 Hz) and with a maximum possible REDOR attenuation of 14.1% as in the trigonal pyramid model. For the two temperatures, summation of the two contributions yields excellent agreement with the experimental data, as shown in Figure 6. This agreement further substantiates the consistency of the entire data set and its interpretation.

$^{29}Si\ \{^{15}N\}$ REDOR in the "hydrated" state (Figure 3, right; 4 °C) shows much smaller dephasing than that observed in the "dry" state (Figure 3, left). This substantial reduction of relative dephasing is a result of several factors. The major one is the higher hydration of the surface; hence, many more surface sites than in the "dry" state are visible to cross-polarization via proximal hydrogen atoms, no longer preferentially selecting for silica sites with bound alanine; this increased visibility of the total surface is straightforwardly verified in view of the 2-fold increase of the total integrated intensity of the hydrated $^{29}Si\ S_0$ spectrum compared to that of the "dry" state. The second factor is due to the 30% reduction of the bound population upon formation of the free population (upon hydration). Lastly, a larger reorientation amplitude of a part of the bound population may further lead to a reduction of the cross-polarization efficiency of adjacent surface sites, hence de-emphasizing binding sites.

Discussion

Our study provides novel insights, with molecular and chemical resolution, of the binding of alanine to a mesoporous silica surface. Importantly, using a very low hydration state as a starting point (<4 H/nm^2), we evidence a single population of surface bound alanine. In spite of the low H atom density, the alanine amine moiety is found protonated/charged ($-NH_3^+$) and facilitates the binding. An additional important observation is that this moiety selects a specific, nonabundant site (*vide infra*) where it is positioned centered above the plane formed by three or four Si surface atoms, with an internuclear $N\cdots Si$ distance of 4.0−4.2 Å. These selected surface binding sites consist predominantly of Si species Q^3, although also Q^4, with a ∼3:1 ratio. This ratio implies that the binding site is one whose binding potential is formed by two to three silanol hydroxyls (Q^3's), ruling out the possibility of binding sites with a single silanol group. Although other studies employed probe molecules to characterize the surface and infer the distance between adjacent silanol sites,[23,52,56−59] this study is the first to report at such detail the *geometry, stoichiometry, and specificity* of a biomolecule, alanine in this case, to the silica surface binding site.

The specificity of the selected surface binding site is further substantiated when considering a simple statistical model (binomial distribution) to assess its occurrence probability within a 3 Å radius circle. Such a radius encircles the bases of both the triangular and square pyramid models. Using the robust silica surface density[53] of 4.6 Si/nm^2 and assuming uniformly distributed surface Si atoms, the following occurrence probabilities emerge: below 1% for circles containing more than four Si atoms; 86%, most probable, for circles with up to two Si atoms; 13%, for circles with three to four Si atoms, as the identified binding sites. Considering the low loading level of alanine (0.2

alanine/nm^2), this indicates that alanine selectively binds to nonabundant surface sites, with a particular geometry and hence with specific functionality.

Furthermore, while the ammonium moiety is anchored, our observations show that the carboxylate end of the surface bound molecule is undergoing rapid, small amplitude reorientation. This clearly indicates that alanine's ammonium, by interacting with 2−3 silanol groups (out of three to four silicon atoms), is responsible for the binding strength and specificity, while the carboxylate moiety has only a small or no contribution. In the "dry" state, all of the above observations were found to be temperature independent (−20 to 20 °C), implying tight binding. These observations elucidate the chemical driving forces that underlie alanine−surface specific interactions. These interactions may be described as a hydrogen bond network between the ammonium hydrogen atoms and the lone pair electrons of the oxygen atoms of the Si−OH. An additional contribution may arise from electrostatic attraction between the positively charged $-NH_3^+$ and a deprotonated, negatively charged silanol moiety $-Si-O^-$ within the group of three to four Si atoms.

Increasing the hydration level unravels the effect of water molecules on binding and eventually dissolution. Earlier studies showed that, upon surface hydration, different sizes of water clusters are formed, and their population distribution and dynamic properties were characterized.[33] At increased hydration, our studies show the formation of differently bound alanine populations. While a surface bound population as in the "dry" state persists at reduced abundance (25% at −10 °C and 10% at 20 °C), an additional bound population is observed (Figure 5). This population is found to experience the same binding stoichiometry and geometry (intermolecular REDOR data); however, the carboxylate end experiences a larger amplitude reorientation. This observation is rationalized by the presence of water molecule(s) that alters the binding potential. However, another population is detected of "free" alanine molecules undergoing rapid isotropic reorientation, attributed to sites with larger water clusters, where alanine dissolution occurred.

The findings of Vega and co-workers who studied the very same system, L-[d_3]alanine loaded on SBA-15, using ^{1}H and dynamic ^{2}H MAS NMR[33] were briefly reviewed in the Introduction. Since the interactions monitored in the two studies differ by 3 orders of magnitude (51 kHz quadrupolar interaction vs ∼200 Hz dipolar coupling), they enable the probing of dynamic processes at different time scales. All rates of dynamic processes reported by monitoring the quadrupolar interaction are fast on the time scale of the dipolar couplings in our study. The two very different time scales render the two studies complementary; however, a few discrepancies are apparent.

Considering the fact that the "dry" state in our study (<4 H/nm^2) is less hydrated than Vega and co-worker's driest state, our observation of a single population of surface bound alanine is in agreement with Vega's description of static population in excess of 80% (∼4 H/nm^2). In the "hydrated" state (6−12 H/nm^2), however, we identify two bound populations (83−60%, temperature dependent) and one free population. The two-site exchange between bound and free populations as observed by Vega is ruled out in our study, since it would have averaged to zero the intermolecular ^{15}N···^{29}Si dipolar coupling of ∼35 Hz; this is clearly not the case. The bound alanine populations (identified in our study) undergoing small and large amplitude anisotropic motions that partially average the intramolecular ^{15}N···^{13}C dipolar coupling of 203 Hz (preserving ∼35 Hz ^{15}N···^{29}Si dipolar coupling) correspond to Vega's "static" population (70−40%) when probed by ^{2}H quadrupolar interaction (51 kHz). The reorientation motions, while sufficient to reduce the intramolecular ^{15}N···^{13}C dipolar coupling of 203 Hz, are too slow to effect the deuterium MAS lineshapes. This implies for the bound molecules a reorientation time scale on the order of $\sim 10^{-3}$ s. However, the discrepancy of our "free" vs Vega and co-worker's exchanging population suggests that a two-site exchange model may be oversimplified.

The current study also reveals that the onset of dynamics and dissolution, as reflected by the averaging of the dipolar interactions, requires a surprisingly small number of water molecules (>6 H/nm^2), hence transforming a surface immobilized alanine into one with isotropic mobility as in solute-like environment. This observation is in full agreement with that of Vega and co-workers.

Conclusions

L-[1-^{13}C,^{15}N]alanine loaded onto SBA-15 mesoporous silica was chosen as a model system for bioorganic−inorganic interfaces and to establish an experimental framework for molecular level characterization. The NMR methodology mainly utilizes inter- and intramolecular dipolar recoupling NMR techniques (REDOR, SLF[PMLG5]).[34,35]

Our solid state NMR study is the first to elucidate the physicochemical principles that underlie the binding specificity of a biomolecule, alanine, to silica surfaces. Our study identified the surface−biomolecule interactions, including the interacting amine moiety of alanine and its protonation state ($-NH_3^+$). The specific surface site of interaction consists of three to four Si functional groups, with 4.0−4.2 Å separation between N···Si atoms. While alanine is surface-anchored via its ammonium group, the carboxylate end was found to undergo rapid, small amplitude librations, hence determining that the ammonium moiety facilitates the binding and its strength.

The experimental data demonstrate both the wealth of accessible, insightful structural−chemical information and the power of our methodological solid state NMR framework. Applying this approach should prove useful for studying interfacial interactions within a broad range of scientific and technological fields.

It is of interest to note that, in contrast to our findings regarding alanine binding, DFT modeling of microsolvated glycine on a silica surface predicts that glycine binds to geminal hydroxyl groups through the carboxylate function, lying parallel to the surface with the $-NH_3^+$ moiety interacting with water molecules.[60−62] We will make use of these solid state NMR tools to investigate experimentally the chemical and physical details of glycine−SBA-15 interactions on an atomic/molecular level in a future study.

Acknowledgment. We thank Prof. Shimon Vega from Weizmann Institute of Science and Prof. Aharon Loewenstein from Technion for fruitful discussions. We acknowledge the partial financial support by the Nevet grant from the Russell Berrie Nanotechnology Institute.

Supporting Information Available: Figures showing characteristic ^{15}N and ^{13}C CPMAS spectra and ^{1}H NMR spectra of [1-^{13}C,^{15}N]alanine loaded on SBA-15. This material is available free of charge via the Internet at http://pubs.acs.org.

References and Notes

(1) Sarikaya, M.; Tamerler, C.; Jen, A. K. Y.; Schulten, K.; Baneyx, F. *Nat. Mater.* **2003**, *2*, 577–585.
(2) Tamerler, C.; Sarikaya, M. *Acta Biomater.* **2007**, *3*, 289–299.

(3) Tamerler, C.; Sarikaya, M. *Philos. Trans. R. Soc. London, Ser. A* **2009**, *367*, 1705–1726.
(4) Ratner, B. D. *Biomaterials science: An introduction to materials in medicine*; Academic Press: San Diego, CA, 1996; pp 1−8.
(5) Paine, M. L.; Snead, M. L. *J. Bone Miner. Res.* **1997**, *12*, 221–227.
(6) Falini, G.; Albeck, S.; Weiner, S.; Addadi, L. *Science* **1996**, *271*, 67–69.
(7) Long, J. R.; Dindot, J. L.; Zebroski, H.; Kiihne, S.; Clark, R. H.; Campbell, A. A.; Stayton, P. S.; Drobny, G. P. *Proc. Natl. Acad. Sci. U.S.A.* **1998**, *95*, 12083–12087.
(8) Long, J. R.; Shaw, W. J.; Stayton, P. S.; Drobny, G. P. *Biochemistry* **2001**, *40*, 15451–15455.
(9) Epstein, J. R.; Biran, I.; Walt, D. R. *Anal. Chim. Acta* **2002**, *469*, 3–36.
(10) Chicurel, M. E.; Dalma-Weiszhausz, D. D. *Pharmacogenomics* **2002**, *3*, 589–601.
(11) Yarmush, M. L.; Jayaraman, A. *Annu. Rev. Biomed. Eng.* **2002**, *4*, 349–373.
(12) Koneracka, M.; Kopcansky, P.; Timko, M.; Ramchand, C. N.; de Sequeira, A.; Trevan, M. *J. Mol. Catal. B: Enzym.* **2002**, *18*, 13–18.
(13) Linssen, T.; Cassiers, K.; Cool, P.; Vansant, E. F. *Adv. Colloid Interface Sci.* **2003**, *103*, 121–147.
(14) Kresge, C. T.; Leonowicz, M. E.; Roth, W. J.; Vartuli, J. C.; Beck, J. S. *Nature* **1992**, *359*, 710–712.
(15) Zhao, D. Y.; Feng, J. L.; Huo, Q. S.; Melosh, N.; Fredrickson, G. H.; Chmelka, B. F.; Stucky, G. D. *Science* **1998**, *279*, 548–552.
(16) Edler, K. J.; Reynolds, P. A.; White, J. W.; Cookson, D. *J. Chem. Soc., Faraday Trans.* **1997**, *93*, 199–202.
(17) Solovyov, L. A.; Kirik, S. D.; Shmakov, A. N.; Romannikov, V. N. *Microporous Mesoporous Mater.* **2001**, *44*, 17–23.
(18) Sauer, J.; Marlow, F.; Schuth, F. *Phys. Chem. Chem. Phys.* **2001**, *3*, 5579–5584.
(19) Edler, K. J.; Reynolds, P. A.; White, J. W. *J. Phys. Chem. B* **1998**, *102*, 3676–3683.
(20) Zhang, J. Y.; Luz, Z.; Goldfarb, D. *J. Phys. Chem. B* **1997**, *101*, 7087–7094.
(21) Ruthstein, S.; Schmidt, J.; Kesselman, E.; Talmon, Y.; Goldfarb, D. *J. Am. Chem. Soc.* **2006**, *128*, 3366–3374.
(22) Taguchi, A.; Schuth, F. *Microporous Mesoporous Mater.* **2005**, *77*, 1–45.
(23) Shenderovich, I. G.; Buntkowsky, G.; Schreiber, A.; Gedat, E.; Sharif, S.; Albrecht, J.; Golubev, N. S.; Findenegg, G. H.; Limbach, H. H. *J. Phys. Chem. B* **2003**, *107*, 11924–11939.
(24) Baccile, N.; Laurent, G.; Bonhomme, C.; Innocenzi, P.; Babonneau, F. *Chem. Mater.* **2007**, *19*, 1343–1354.
(25) Pizzanelli, S.; Kababya, S.; Frydman, V.; Landau, M.; Vega, S. *J. Phys. Chem. B* **2005**, *109*, 8029–8039.
(26) Gibson, J. M.; Popham, J. M.; Raghunathan, V.; Stayton, P. S.; Drobny, G. P. *J. Am. Chem. Soc.* **2006**, *128*, 5364–5370.
(27) Gibson, J. M.; Raghunathan, V.; Popham, J. M.; Stayton, P. S.; Drobny, G. P. *J. Am. Chem. Soc.* **2005**, *127*, 9350–9351.
(28) Shaw, W. J.; Long, J. R.; Campbell, A. A.; Stayton, P. S.; Drobny, G. P. *J. Am. Chem. Soc.* **2000**, *122*, 7118–7119.
(29) Jaeger, C.; Groom, N.; S. Bowe, E.; Horner, A.; Davies, M. E.; Murray, R. C.; Duer, M. J. *Chem. Mater.* **2005**, *17*, 3059–3061.
(30) Maltsev, S.; Duer, M. J.; Murray, R. C.; Jaeger, C. *J. Mater. Sci.* **2007**, *42*, 8804–8810.
(31) Zhao, D. Y.; Huo, Q. S.; Feng, J. L.; Chmelka, B. F.; Stucky, G. D. *J. Am. Chem. Soc.* **1998**, *120*, 6024–6036.
(32) Beck, J. S.; Vartuli, J. C.; Roth, W. J.; Leonowicz, M. E.; Kresge, C. T.; Schmitt, K. D.; Chu, C. T. W.; Olson, D. H.; Sheppard, E. W.; Mccullen, S. B.; Higgins, J. B.; Schlenker, J. L. *J. Am. Chem. Soc.* **1992**, *114*, 10834–10843.
(33) Amitay-Rosen, T.; Kababya, S.; Vega, S. *J. Phys. Chem. B* **2009**, *113*, 6267–6282.
(34) Gullion, T.; Schaefer, J. *J. Magn. Reson.* **1989**, *81*, 196–200.
(35) Hester, R. K.; Ackerman, J. L.; Neff, B. L.; Waugh, J. S. *Phys. Rev. Lett.* **1976**, *36*, 1081–1083.
(36) Gullion, T.; Schaefer, J. *Adv. Magn. Opt. Reson.* **1989**, *13*, 57.
(37) Veshtort, M.; Griffin, R. G. *J. Magn. Reson.* **2006**, *178*, 248–282.
(38) Massiot, D.; Fayon, F.; Capron, M.; King, I.; Calvé, S. L.; Alonso, B.; Durand, J.; Bujoli, B.; Gan, Z.; Hoatson, G. *Magn. Reson. Chem.* **2002**, *40*, 70–76.
(39) Vinogradov, E.; Madhu, P. K.; Vega, S. *Chem. Phys. Lett.* **1999**, *314*, 443–450.
(40) Vinogradov, E.; Madhu, P. K.; Vega, S. *J. Chem. Phys.* **2001**, *115*, 8983–9000.
(41) Vinogradov, E.; Madhu, P. K.; Vega, S. *Chem. Phys. Lett.* **2002**, *354*, 193–202.
(42) Leskes, M.; Madhu, P. K.; Vega, S. *Chem. Phys. Lett.* **2007**, *447*, 370–374.
(43) Leskes, M.; Madhu, P. K.; Vega, S. *J. Chem. Phys.* **2006**, 125.
(44) Bork, V.; Gullion, T.; Hing, A.; Schaefer, J. *J. Magn. Reson.* **1990**, *88*, 523–532.
(45) deAzevedo, E. R.; Saalwachter, K.; Pascui, O.; de Souza, A. A.; Bonagamba, T. J.; Reichert, D. *J. Chem. Phys.* **2008**, *128*, 104505.
(46) Peacor, D. R. *Z. Kristallogr.* **1973**, *138*, 274–298.
(47) Chuang, I. S.; Maciel, G. E. *J. Phys. Chem. B* **1997**, *101*, 3052–3064.
(48) Kobayashi, T.; DiVerdi, J. A.; Maciel, G. E. *J. Phys. Chem. C* **2008**, *112*, 4315–4326.
(49) Lopez, J. J.; Mason, A. J.; Kaiser, C.; Glaubitz, C. *J. Biomol. NMR* **2007**, *37*, 97–111.
(50) Schmidt, A.; Mckay, R. A.; Schaefer, J. *J. Magn. Reson.* **1992**, *96*, 644–650.
(51) Schmidt, A.; Kowalewski, T.; Schaefer, J. *Macromolecules* **1993**, *26*, 1729–1733.
(52) Shenderovich, I. G.; Mauder, D.; Akcakayiran, D.; Buntkowsky, G.; Limbach, H. H.; Findenegg, G. H. *J. Phys. Chem. B* **2007**, *111*, 12088–12096.
(53) Zhuravlev, L. T. *Colloids Surf., A* **2000**, *173*, 1–38.
(54) Lehmann, M. S.; Koetzle, T. F.; Hamilton, W. C. *J. Am. Chem. Soc.* **1972**, *94*, 2657–2660.
(55) Goetz, J. M.; Schaefer, J. *J. Magn. Reson.* **1997**, *129*, 222–223.
(56) Buntkowsky, G.; Breitzke, H.; Adamezyk, A.; Roelofs, F.; Emmler, T.; Gedat, E.; Grunberg, B.; Xu, Y.; Limbach, H. H.; Shenderovich, J.; Vyalikh, A.; Findenegg, G. *Phys. Chem. Chem. Phys.* **2007**, *9*, 4843–4853.
(57) Gedat, E.; Schreiber, A.; Albrecht, J.; Emmler, T.; Shenderovich, I.; Findenegg, G. H.; Limbach, H. H.; Buntkowsky, G. *J. Phys. Chem. B* **2002**, *106*, 1977–1984.
(58) Grunberg, B.; Emmler, T.; Gedat, E.; Shenderovich, J.; Findenegg, G. H.; Limbach, H. H.; Buntkowsky, G. *Chem.—Eur. J.* **2004**, *10*, 5689–5696.
(59) Pan, V. H.; Tao, T.; Zhou, J. W.; Maciel, G. E. *J. Phys. Chem. B* **1999**, *103*, 6930–6943.
(60) Lomenech, C.; Bery, G.; Costa, D.; Stievano, L.; Lambert, J. F. *ChemPhysChem* **2005**, *6*, 1061–1070.
(61) Costa, D.; Lomenech, C.; Meng, M.; Stievano, L.; Lambert, J. F. *THEOCHEM* **2007**, *806*, 253–259.
(62) Costa, D.; Tougerti, A.; Tielens, F.; Gervais, C.; Stievano, L.; Lambert, J. F. *Phys. Chem. Chem. Phys.* **2008**, *10*, 6360–6368.

JP100114V